Study of Contact Strength, Tooth Wear and Metal-Polymer Life of Worm Gears

Myron Czerniec[1], Antoni Świć[2*]

[1] Aerospace Faculty, National Aviation University, Liubomyra Huzara Ave. 1, 03058 Kyiv, Ukraine
[2] Lublin University of Technology, ul. Nadbystrzycka 36, 20-388 Lublin, Poland

ABSTRACT
This paper presents results of a study investigating worm gears consisting of polymer worm wheels and steel involute and Archimedes worms. The author uses his own calculation method to predict polymer wheel wear, gear life and maximum contact pressure in mesh. The effect of tooth correction and wear on gear life and contact pressure is considered. Cases of double and triple tooth engagement are analysed. The worm wheel is made of non-reinforced polyamide PA6. Quantitative and qualitative relationships are established between the maximum initial contact pressure along tooth profile and the tooth correction coefficient. Tooth wear causes a considerable decrease in contact pressure, with the highest decrease observed at the exit of engagement. The maximum contact pressure is generated at the exit of engagement. The same trend is observed for tooth wear. The minimum gear life is observed at the exit of engagement. It increases linearly with increasing the coefficient of tooth correction. The gear life significantly increases (by approx. 56%) in triple tooth engagement compared to double tooth engagement.

Keywords: metal-polymer worm gear, PA6 polyamide, PA6+30GF, involute and Archimedes worm gears, calculation method, tooth correction, contact pressure, tooth wear and life.

INTRODUCTION

Worm gears with metal wheels and worms have many different applications in machine building and other industrial areas. These toothed gears have threaded axes where meshing occurs by sliding friction. The most popular are involute and Archimedes worm gears. For their long-lasting and reliable operation, it is necessary to ensure boundary lubrication. When lubricant degrades and required lubrication conditions are not met, there occurs galling and the gear is no longer capable of operation. For this reason, worm gears cannot be used under non-lubricating conditions, as this would cause dry friction. To overcome this problem, such gears can be made as a combination of metal (worm) and polymer (worm wheel). Worm wheels can be made of PA polyamides and their composites as well as POM polyacetals. Metal-polymer (MP) worm gears are used in various areas of human activity. They can be operated

under low loads and have relatively short operating periods.

The development of methods for estimating load capacity, tooth wear and service life of metal-on-metal and metal-polymer worm gears is of vital importance. Load capacity (contact strength) of metal worm gears is determined in compliance with different standards (ISO / TR 14521: 2010, DIN 3396, BS 721, AGMA 6034, etc.). There exist only very few studies investigating the problem of contact pressure [12, 20, 21]. In [13, 20] the effect of load on pressures under elastohydro-dynamic lubrication (EHDL) was investigated. Studies [12, 13, 23] present methods for calculating contact pressures. The above-mentioned methods can be used for investigating MP worm gears albeit with some limitations. However, the literature provides no information about such investigations.

The application of computational and numerical methods for estimating wear and tribological

durability of metal worm gears is reported in very few studies [19, 22, 24]. Studies [6, 18, 27] propose methods for investigating gear tooth wear according to Archard's law of abrasive wear with EHDL. The method for estimating wear and life of worm gear proposed in [19] is based on empirical formulas. The numerical method of tooth wear estimation considering lubricant film thickness proposed in [2, 6, 13] is also based on the Archard wear law. However, it should be emphasized that this wear law does not reflect wear conditions. The above-mentioned methods do not take into account the effects of wheel tooth correction and their wear on the load capacity and service life of the gear. These effects have only been investigated by the author in his previous studies [2, 4, 6]. In [2, 4] in gears with two-pair meshing, and in [6] – with two- and three-pair.

The literature review shows that there are no studies investigating the tribological behaviour of MP worm gears, and thus methods for estimating their wear and life at friction with lubrication and under dry friction conditions. The existing studies [9, 11, 15, 26] investigate other aspects of these gears. A study [7, 16] proposes a method for calculating load on involute worm gears with localized tooth contact. Elastic strains of gear teeth and bending stresses under different loading conditions were determined by geometric modelling. A method for estimating quasi-static loading of MP worm gears (steel worm – polyamide worm wheel) is presented in [8, 11 15]. In [16] are presented results obtained for seven different types of PA polyamide: PA6, PA6+15GF, PA6+30GF, PA66, PA66+30GF, PA66+60GF, which is widely used as a material for worm gears in cars. Their temporary tensile strength Young's modulus, abrasive wear resistance under dry friction conditions, and impact strength were determined. In [17] von Mises stresses in a worm wheel made of PA66+GF (25 wt.% and 50 wt.% fiberglass) were investigated. Experiments were conducted to determine the life of a prototype worm gear made of these polymer composites. A new method for determining the service life of MP worm gears was presented in [14, 15, 25].

Experimental results of pin-on-disk tests conducted under fry friction conditions for polyamides and their composites in combination with steel [10, 14, 17] have been reported in the literature. In [17] a combination of PA6 polyamide and AISI 02 steel was investigated. Results of numerous studies (over 20) conducted on reinforced and non-reinforced polymeric materials are reported in [14]. Studies [1, 16, 18] investigated the tribological behaviour of PA6 polyamide and steel under dry friction conditions and under friction with lubrication.

This paper presents results of a study investigating the effect of meshing conditions, tooth correction and wear on the service life and load-bearing capacity of an MP worm gear with an involute and Archimedes worm. The worm wheel was made of PA6 polyamide and PA6+30GF.

CALCULATION METHOD FOR MP WORM GEARS

The proposed modified calculation method for MP worm gears (Fig.1) is based on the previous method developed for metal worm gears [2, 3, 5, 6] that are operated under boundary friction or EHDL conditions. The proposed calculation method is based on phenomenological method for estimating material wear at sliding friction [1, 4, 7] due to fatigue wear. The application of this friction mechanism for materials such as polymers is more justified than the use of the adhesive-abrasive wear mechanism according to the Archard linear wear law.

MP worm gears are usually operated under dry friction conditions, because polyamides and polyacetals used for worm wheels have very good lubricating properties. Nevertheless, these gears can also be used with lubrication.

Below is shown a modified calculation method for MP worm gears. The function of linear wear of worm wheel teeth 2 during engagement

Fig. 1. Metal-polymer involute worm gear

under initial (constant) contact pressure has the following form:

$$h_{2j}' = \frac{v_j t_j' \left(f p_{j\,max}^{(w)} \right)^{m_2}}{C_2 \left(\tau_{s2} \right)^{m_2}} \qquad (1)$$

where: $t_j' = 2b_j / v_j$ is the time of contact of the elements in mesh at *j*-th point on friction path with a length of *2b_j*,
$2b_j^{(w)} = 2.256\sqrt{\Theta N' \rho_j / bw}$ is the contact area width based on the Hertz theory of contact stresses,
v_j is the sliding velocity at a point *j* of engagement at a height of worm threads in the axial section,
$w = 1, 2, 3$ is the number of pairs of teeth carrying the load,
f is the sliding friction factor,
C,m are the indicators of abrasive wear resistance of materials of the worm teeth and worm wheel, determined via experiments conducted according to the method described in [19],
$\tau_{S2} = 0.5R_m$ is the shear strength of the polymer
R_m is the temporary tensile (compression) strength of the polymer
$p_j^{(w)}{}_{max}$ is the maximum contact pressure,
$\theta = \left(1-v_1^2\right)/E_1 + \left(1-v_2^2\right)/E_2$,
v_k, E_k are respectively Poisson's ratio and Young's modulus for the material of the worm ($k = 1$) and worm wheel ($k = 2$),
b is the width of the worm wheel,
j denotes points on the worm thread profile and worm wheel teeth.

Maximum contact pressures $p_j^{(w)}{}_{max}$ are determined using the Hertz equation

$$p_{j\,max}^{(w)} = 0,564\sqrt{N'/w\theta\rho_j b} \qquad (2)$$

where: N' is the tooth load,
ρ_j is the equivalent curvature radius at a point *j* of engagement.

$$N' = \frac{2T}{d_1 \cos\alpha_{pxj} \sin(\gamma + \rho')} \qquad (3)$$

where: $T = 9550\cdot 10^3 (N/n_1)$ is the torque on the wormshaft,
n_1 is the number of revolutions of the worm,
$\rho' = arctg\left(f / \cos\alpha \right)$ is the apparent friction angle,
N is the power transmitted by the gear.

The equivalent curvature radius ρ_j at a point *j* of engagement is calculated from profile curvature radii of the worm ρ_{1j} and worm wheel ρ_{2j}

$$\rho_j = \frac{\rho_{1j}\rho_{2j}}{\rho_{1j} + \rho_{2j}} \qquad (4)$$

Hence,
- *for an involute worm gear*

$$\rho_{1j} = -\frac{r_b tg\alpha_{cj}}{\cos^3\alpha_{pxj} tg\gamma_b \cos^2\left(\alpha_{cj} + \varepsilon_j\right)}$$

$$\rho_{2j} = \frac{\rho_{1j}r_2 \sin\alpha_{pxj} + \rho_{1j}e_{pAj} - e_{pAj}^2}{r_2 \sin\alpha_{pxj} + \rho_{1j} - e_{pAj}} \qquad (5)$$

- *for an Archimedes worm gear with trapezoid profile it is necessary to consider*

$$\rho_{2j} = (\frac{d_2}{2}\sin\alpha_{xj} + e_{pAj}). \qquad (6)$$

where: $r_b = 0,5d_1\cos\alpha_c$ is the radius of the main cylinder of the worm,
$\alpha_{cj} = arctg\frac{\sqrt{x^2 - r_b^2}}{r_b}$ is the end-face pressure angle at *j*-th point,
$\alpha_{pxj} = arctg\left(-tg\gamma_b\frac{\sqrt{x^2 - r_b^2}}{x}\right)$ is the angle of a tangent to the profile at *j*-th point on the worm tooth profile in the axial section, relative to the axis of the worm,
x is the distance of *j*-th point from the axis of the worm in the axial section,
γ_b is the base lead angle,
$d_1 = qn$ is the pitch diameter of the worm,
$q = 2\left(1+\sqrt{z_2}\right)$ is the diameter quotient of the worm gear,

$r_2 = 0,5z_2m$, $r_2 = 0,5d_2$ is the pitch radius of the worm wheel,

$z_2 = uz_1$ is the number of teeth on the worm wheel,

u is the gear ratio,

z_1 is the number of threads on the worm,

m is the module of meshing,

$e_{pAj} = \dfrac{r_1 - x}{\sin\alpha_{pxj}}$ is the distance of *j*-th point from a contact point measured along contact section,

$r_1 = 0,5d_1$ is the pitch radius of the worm,

$\varepsilon_j^0 = \dfrac{180}{\pi}\dfrac{\sqrt{x^2 - r_b^2}}{r_b}$ is the angular coordinate.

The *x* coordinate values along the worm thread height range $x_A < x < x_B$. Accordingly, $x_A = r_{f_1} + 0,2m$, $x_B = r_{a_1}$. The x_A coordinate denotes the entry of engagement while the x_B coordinate marks the exit of engagement. The section $[x_A, x_B]$ was proportionally divided into several smaller sections with contact points 1, 2, 3, 4, 5 (Fig. 2).

Geometrical parameters of the gear are:

$r_{f_1} = 0,5\left(d_1 - 2h_{f_1}\right), h_{f_1} = 1,2m$ (for $\gamma \le 15°$),

$h_{f_1} = 1,2m_n$ (for $\gamma \rangle 15°$);

$r_{a_1} = 0,5\left(d_1 + 2h_{a_1}\right), h_{a_1} = m$ (for $\gamma \le 15°$),

$h_{a_1} = m_n$ (for $\gamma \rangle 15°$);

$tg\gamma = mz_1 / d_1$, $b = 2m\sqrt{q+1}$.

Other parameters:

- f*or an involute worm gear:*

$r_b = 0,5d_1\cos\alpha_c$, $tg\alpha_c = tg\alpha / \sin\gamma$,

$\alpha = 20°$, $\alpha_{cj} = arctg\dfrac{\sqrt{x^2 - r_b^2}}{r_b}$,

$\alpha_{pxj} = arctg\left(-tg\gamma_b\dfrac{\sqrt{x^2 - r_b^2}}{x}\right)$,

$tg\gamma_b = \dfrac{mz_1}{d_1\cos\alpha_c}$, $\varepsilon_j = \dfrac{180}{\pi}\dfrac{\sqrt{x^2 - r_b^2}}{r_b}$.

- f*or an Archimedes worm gear:*

$\alpha_{pxj} = arctg(-tg\alpha_{xj})$, $tg\alpha_{xj} = \dfrac{180}{\pi}\dfrac{mz_1}{2x}$.

The total sliding velocity during engagement

$$v_j = \sqrt{(v'_j)^2 + (v''_j)^2} \qquad (7)$$

where: v'_j is the velocity due to rotational motion of the worm (helical component),

v''_j is the velocity of a contact point along the tooth profile (velocity component resulting from rotating about the teeth).

Hence

$$v'_j = \frac{\omega_1 x}{\cos\gamma_A}, \; v''_j = e_{pAj}\omega_2 \qquad (8)$$

where: $tg\gamma_A = mz_1 / 2x$

$\omega_1 = \pi n_1 / 30$, $\omega_2 = \omega_1 / u$ are the angular velocities of the worm and worm wheel, respectively.

The gear life t_* for a given permissible wear h_{2*} of worm wheel teeth, assuming that $p_j^{(w)}{}_{max} = const$, is expressed as:

$$\ddot{t}_* = \left(\bar{h}_{2*} / \bar{h}_{2j}\right) \qquad (9)$$

where: $\bar{h}_{2j} = 60n_2 h'_{2j}$, $n_2 = n_1 / u$ denote the wear of the worm wheel teeth per one hour.

The application of gear tooth correction leads to changes in interaxial distance and reference diameter

$$a_{wk} = a_w + x_2 m, \; d_{w1} = d_1 + x_2 m \qquad (10)$$

where: $a_w = r_1 + r_2$ is the interaxial distance in a non-corrected gear,

x_2 is the tooth correction coefficient.

Now using Equation (3) which describes tooth load and the equation describing e_{pAj} it is necessary to deduce a radius of $r_{w1} = 0.5d_{w1}$.

Worm wheel tooth correction does not cause any changes in worm dimensions.

Worm wheel teeth undergo wear with operation, which leads to reduction in maximum contact pressure and, as a result, to increased gear life. This relationship must therefore be taken into consideration. The change in the initial curvature
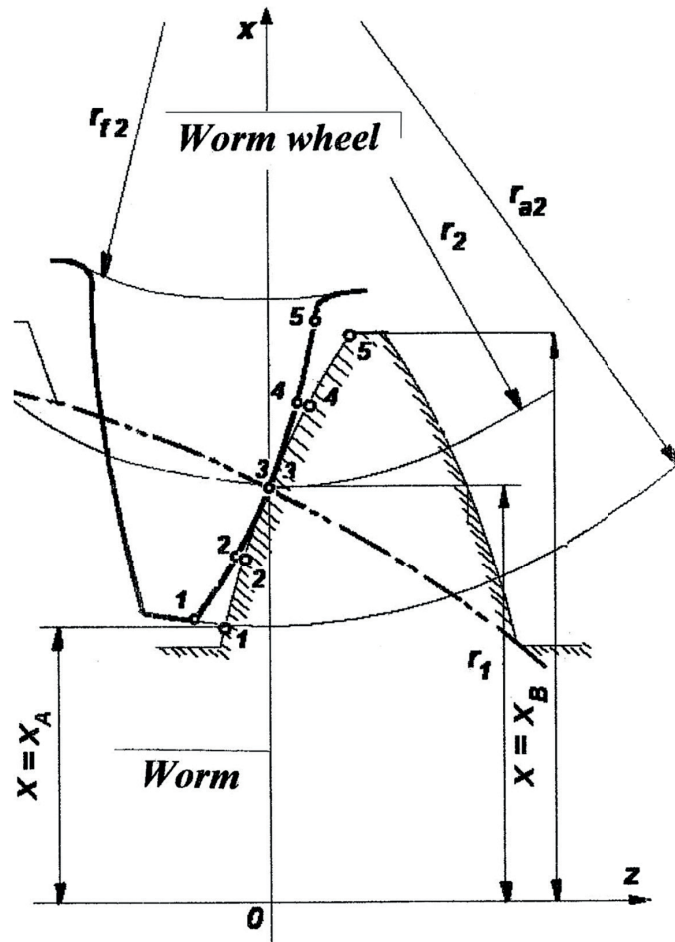
Fig. 2. Location of contact points

radius ρ_{2j} of the worm wheel tooth profile is determined according to [2] as

$$\rho_{2jh} = \rho_{2j} + \lambda_h \sum^{n_2} h'_{2jn} \qquad (11)$$

where: λ_h his the wear rate coefficient,
h'_{2jh} is the variable unit wear in every meshing cycle.

Linear wear of the worm wheel teeth causing changes in ρ_{2j} (6), $t'_j = 2b_j / v_j$, $p_{j\max}$ (2),

for the number n_{2*} of wheel revolutions, results in the permissible wear h_{2*} of the wheel teeth,

$t'_{jh} = 2b_{jh} / v_j$ is the variable tribocontact time after every meshing cycle.

Tooth wear occurring in every revolution of the gear leads to an increase in the initial curvature radius ρ_{2j} of the worm wheel tooth profile. As a result, the maximum contact pressure

continues to decrease while contact area width increases. Therefore:

$$p_{jh\max} = 0,564\sqrt{N'/bw\theta\rho_{jh}} ,$$
$$2b_{jh} = 2,256\sqrt{\theta N'\rho_{jh}/bw} \qquad (12)$$

Since wear of the steel worm can be omitted, the variable curvature radii are:

$\rho_{jh} = \dfrac{\rho_{1j}\rho_{2jh}}{\rho_{1j} + \rho_{2jh}}$ is the equivalent curvature

radius in an involute worm gear;

$\rho_{jh} = \rho_{2jh}$ is the curvature radius in an Archimedes worm gear.

Therefore, Equation (1) describing the unit linear wear of worm wheel teeth in every interaction is

$$h'_{2jh} = \frac{v_j t'_{jh} \left(f p^{(w)}_{jh\max} \right)^{m_2}}{C_2 \left(\tau_{s2} \right)^{m_2}} \qquad (13)$$

The above equation requires a relatively long time to calculate the parameters h'_{2jh}, ρ_{2jh}, ρ_{jh}, $p_{jh\max}$, $2b_{jh}$, t'_{jh}. To shorten the computations, a block-cumulative procedure was employed. For a given number of wheel revolutions n_2 (interaction block B), contact pressure $p_{j\max}$ and $2b_j$, t'_j, h'_{2j} are constant (as shown above in the simplified calculation model). Since tooth wear causes changes in tooth profile radius, determined in accordance with (11), the initial parameters $p_{j\max}$, $2b_j$, t'_j, h'_{2j} undergo changes, too. These changes are taken into consideration in every successive block. The procedure is repeated cyclically until the assumed permissible wear is achieved at a given point on tooth profile. The time of calculations can be shortened proportionally to the size of an interaction block. Equation (11) takes the form:

$$\rho_{2jh} = \rho_{2j} + \lambda_h \sum^{B} h'_{2jn} \qquad (14)$$

According to the rotary-cumulative and block-cumulative procedure the total linear wear h_{2jn} of worm wheel teeth is calculated with the equation

$$h_{2jn} = \sum_{1}^{n_{2*}} h'_{2jn},$$
$$h_{2jn} = \sum_{1}^{B} h_{2jB} \qquad (15)$$

where: $h_{2jB} = \sum h'_{2j}$ denotes the wear of gear teeth in every block with variable meshing conditions.

Gear life for the total number of worm wheel revolutions n_{2*} resulting in reaching the permissible tooth wear h_{2*} is calculated as:

$$t_* = n_{2*} / 60n_2 \qquad (16)$$

RESULTS AND DISCUSSION

The following were determined: the initial contact pressure $p_{j\max}$ and its variation $p_{jh\max}$ due to tooth wear, the total linear wear h_{2*} at selected points on the worm wheel tooth profile, the linear wear $\overline{h}_2$ at the contact point most

susceptible to wear within one hour of gear operation, and the minimum gear life $t_{\min}$. Cases of double and triple tooth engagement were analysed ($w = 2$, $w = 3$). Worm wheel tooth correction was taken into consideration. Calculations were made for two meshing models: for $p_{j\max} = const$, i.e. without considering the effect of tooth wear on contact conditions, and for $p_{j\max} = var$, i.e. considering the effect of tooth correction.

The calculations were made using the following load-related, kinematic, geometrical, material and tribological parameters:

$N = 1.0$ kW, $n_1 = 700$ rpm, $m = 4$ mm, $z_1 = 1$, $u = 25$, $q = 12$, $b = 26.84$ mm; material of the worm: normalized C45 steel (HRC 45) described by $E_1 = 2.1 \times 10^5$ MPa, $\nu_1 = 0.3$; materials of the worm wheel: PA6 polyamide described by $E_2 = 2000$ MPa, $\nu_2 = 0.4$; $C_2 = 1.34 \times 10^6$, $m_2 = 1.15$; $\tau_{s2} = 40$ MPa, $f = 0.21$; PA6+30GF described by $E_2 = 2700$ MPa, $\nu_2 = 0.41$; $C_2 = 1.88 \times 10^6$, $m_2 = 1.15$; $\tau_{s2} = 50$, $f = 0.3$; $h_{2*} = 0.5$ mm; $x_2 = 0, 0.5, 1.0$; $\ddot{e}_h = 100$, $B = 5$ $(60\ddot{u}_1) = 8400$ revolutions (5 hours of operation). The wear characteristics C_2, m_2 of polymeric materials and the sliding friction coefficient f were determined via the author's own pin-on-disk tests conducted under dry friction conditions. Dry friction occurs in the tested gears.

The following contact points j on the worm wheel tooth profile were selected: $j = 1 \rightarrow x = x_A = 18$ mm (entry of engagement), $j = 2 \rightarrow x = 20$ mm, $j = 3 \rightarrow x = 22$ mm, $j = 4 \rightarrow x = 24$ mm, $j = 5 \rightarrow x = x_B = 26$ mm (exit of engagement).

Results are given in Figs. 3 – 9. Figs. a) show results obtained for an MP involute worm gear while Figs. b) – for an MP Archimedes worm gear. Figs. 3 and 4 show changes in the maximum initial contact pressure $p_{j\max}^{(w)}$ along the tooth profile as a result of correction. Also, changes in contact pressure induced by tooth wear are presented.

The contact pressure is the lowest at the entry of engagement while its highest values are located at the exit of engagement. It increases up to 2.067 times. A similar qualitative change can also be observed along tooth profile. The increase value depends on the tooth correction coefficient x_2. Tooth correction reduces the pressure by approx. 1.55 times. The contact pressure in the MP involute worm gear is up to 1.34 times higher than that in the Archimedes worm gear, particularly at the
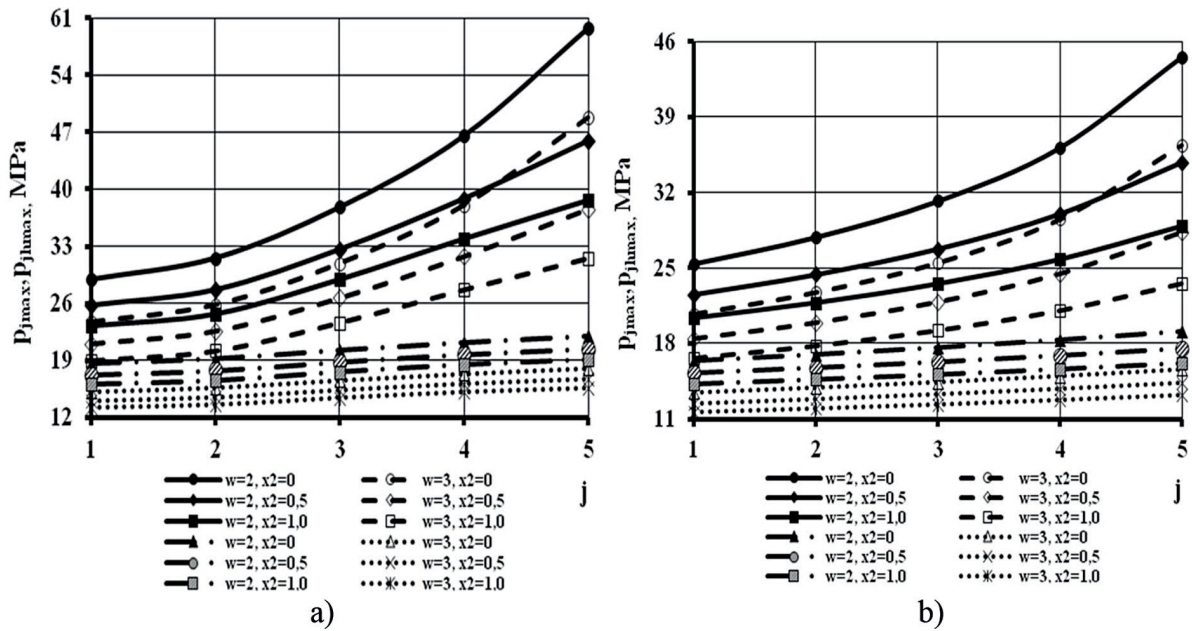
Fig. 3. Wear-induced changes in maximum contact pressure along tooth profile in a PA6 wheel
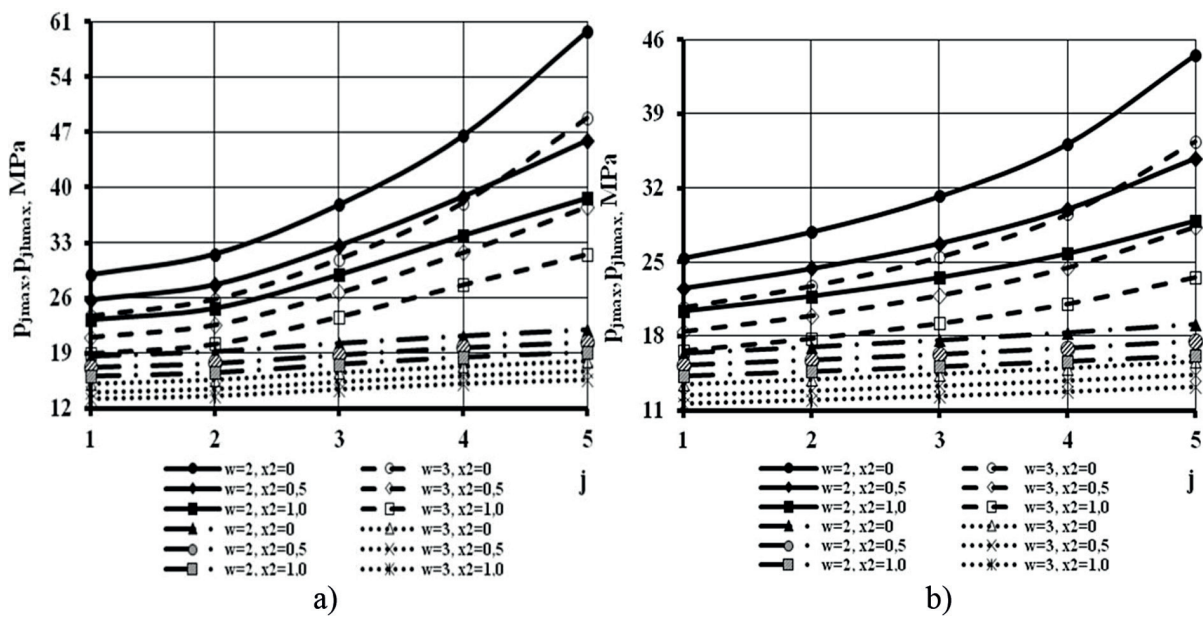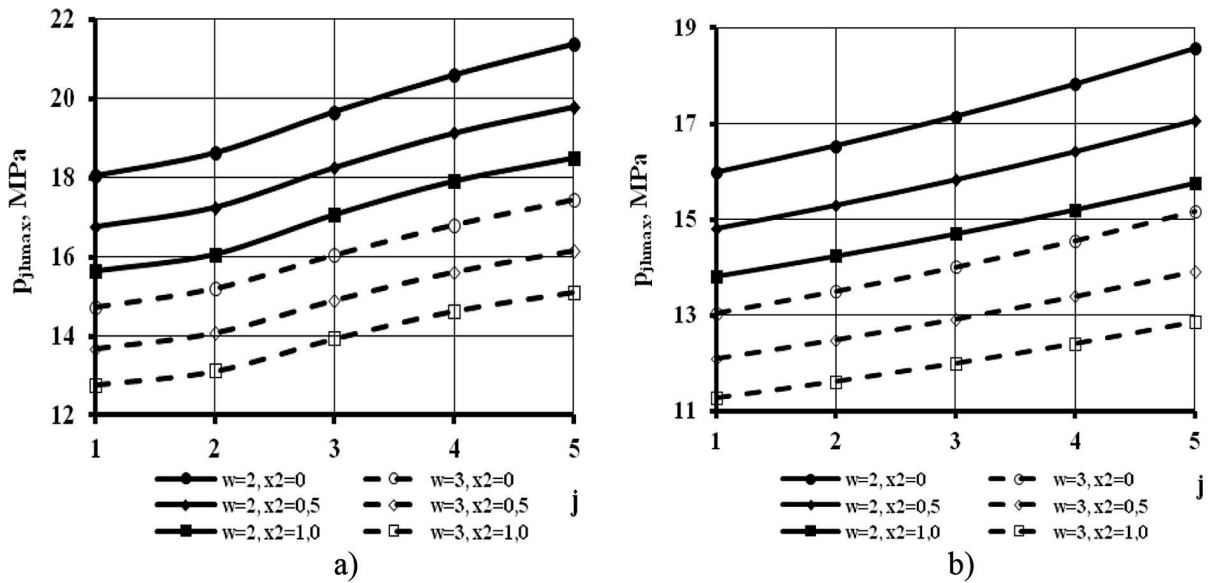

Fig. 4. Wear-induced changes in maximum contact pressure along tooth profile in a PA6+30GF wheel

exit of engagement. The maximum contact pressure in the gear with a PA6 worm wheel is up to 1.03 times lower than that obtained for the gear with a PA6+30GF wheel.

It can be observed that the maximum contact pressure $p_{j\max}^{(w)}$ significantly decrease due to wear of the worm wheel teeth. The observed changes in pressure are illustrated in Figs. 5 and 6.

Figs. 7 and 8 show the effect of worm wheel tooth correction on the initial maximum contact pressure $p_{5\max}^{(w)}$ and variations in $p_{5h\max}^{(w)}$ due to tooth wear at the exit of engagement ($j = 5$).

Increasing the number of teeth in mesh from $w = 2$ to $w = 3$ leads to a decrease in the pressure by up to 1.22 times. This demonstrates a close relationship between tooth wear and reduction in initial pressure at the exit of engagement point (it is reduced up to 2.06 times).

Between the entry and exit of engagement, the pressures $p_{jh\max}^{(w)}$ increase in a linear fashion.

The minimum gear life $t_{\min}$ (p_j = const) and $t_{B\min}$ (p_j = var), considering the effect of tooth correction, is shown in Figs. 9 and 10.

Fig. 5. Wear-induced changes in maximum contact pressure along tooth profile in a PA6 wheel
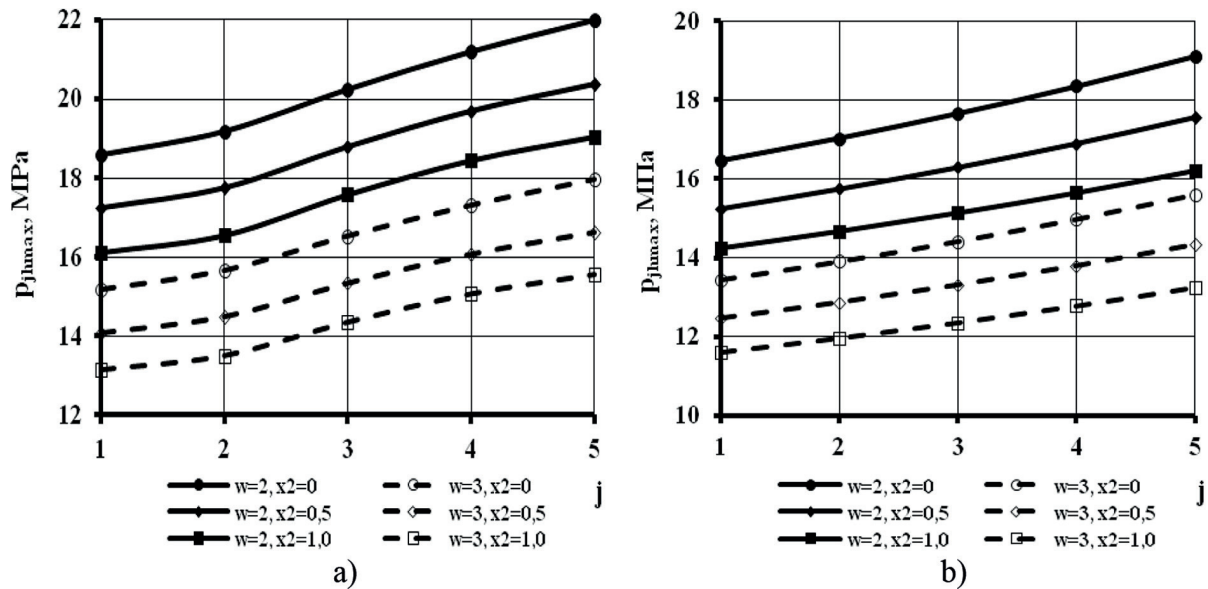

Fig. 6. Wear-induced changes in maximum contact pressure along tooth profile in a PA6+30GF wheel

Tooth correction leads to a linear increase in minimum gear life (at $j = 5$). The life of the gear after tooth correction is about 1.2 times longer than that of the gear with non-corrected teeth for p_j = const (t_{min}) and about 1.25 times for p_j = var (t_{Bmin}) due to tooth wear. The minimum gear life is observed at the exit of engagement. The life of the Archimedes worm gear is approx. 1.28 times longer than that of the involute worm gear. The life of the gear with a PA6+30GF wheel is approx. 1.5 times longer than that of the gear with a PA6 wheel. It can also be observed that the gear life greatly depends on the tooth engagement type (by approx. 1.55 times).

The linear wear h_{2j} of gear teeth along their profile is shown in Figs. 11 and 12.

Lower wear is located at the entry of engagement while the permissible wear $h_{2*} = 0.5$ mm can be observed at the exit of engagement. The wear increases linearly along the tooth profile.

The linear wear $\overline{h}_{2(5)}$ of corrected teeth at the exit of engagement per one hour of operation is shown in Figs. 13 and 14. The results show the final hour of gear operation for the models p_j = const and p_j = var.

Tooth correction leads to a decrease in the linear wear $\overline{h}_{2(5)}$ (at exit of engagement). The decrease depends on the type of gear and meshing as well as worm wheel polymeric material.
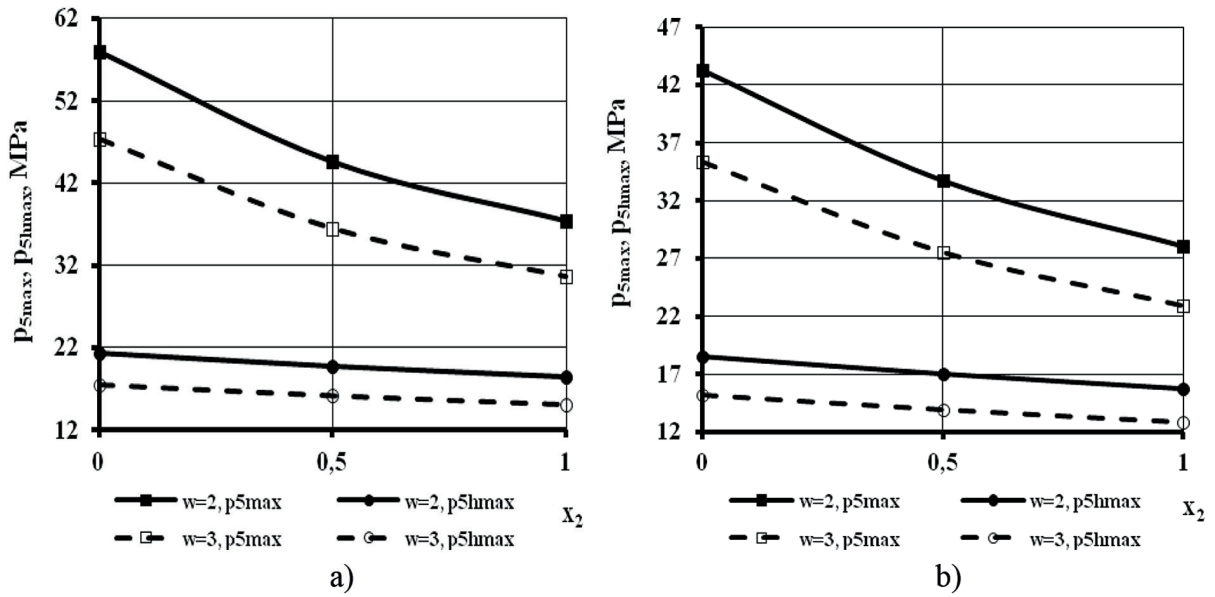
Fig. 7. Effect of PA6 wheel tooth correction on maximum contact pressure
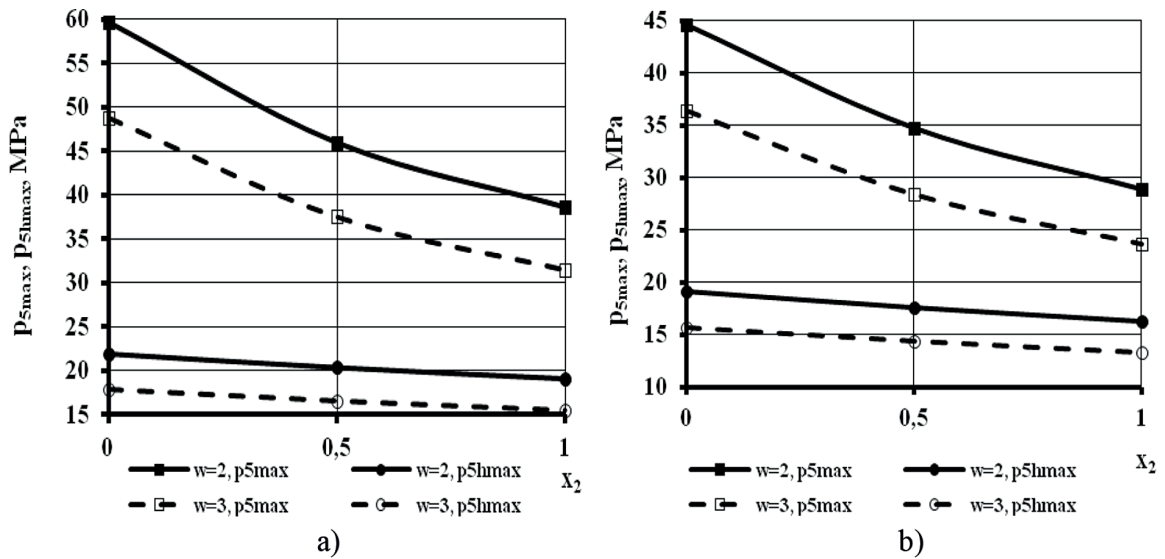

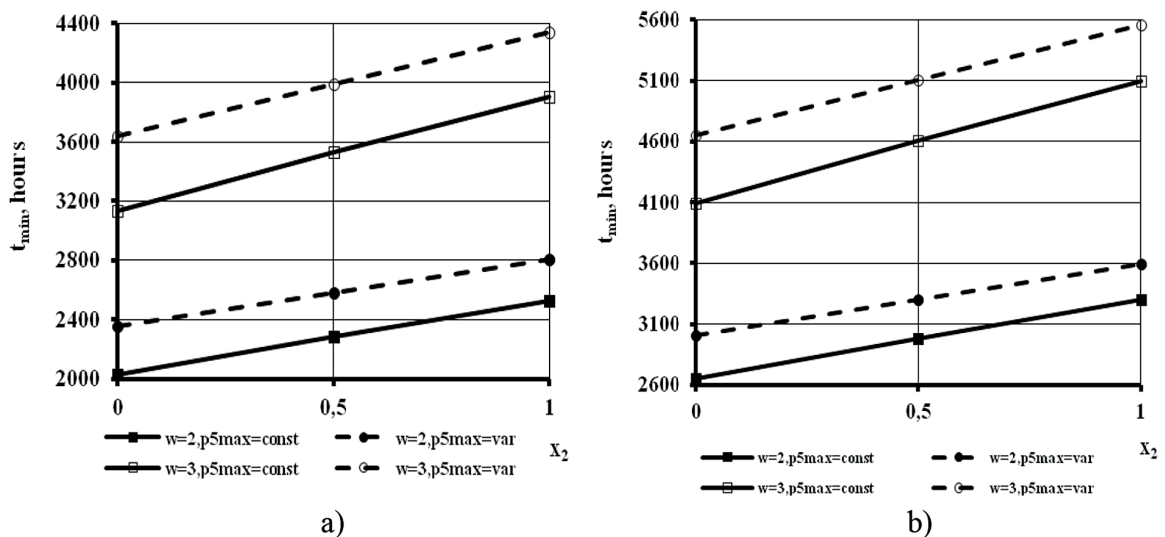**Fig. 8.** Effect of PA6+30GF gear tooth correction on maximum contact pressure

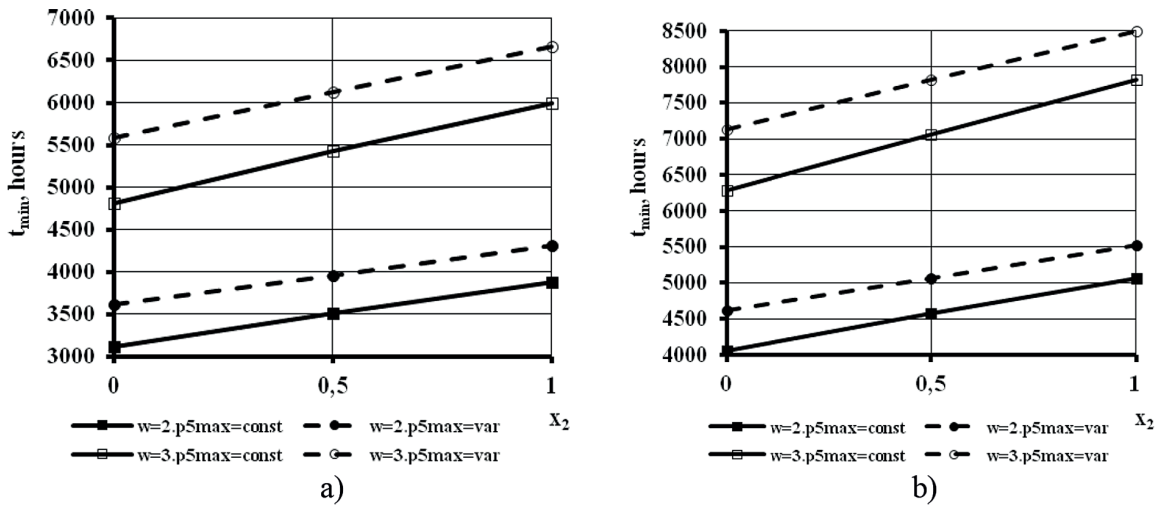

Fig. 9. Minimum life of a PA6 gear

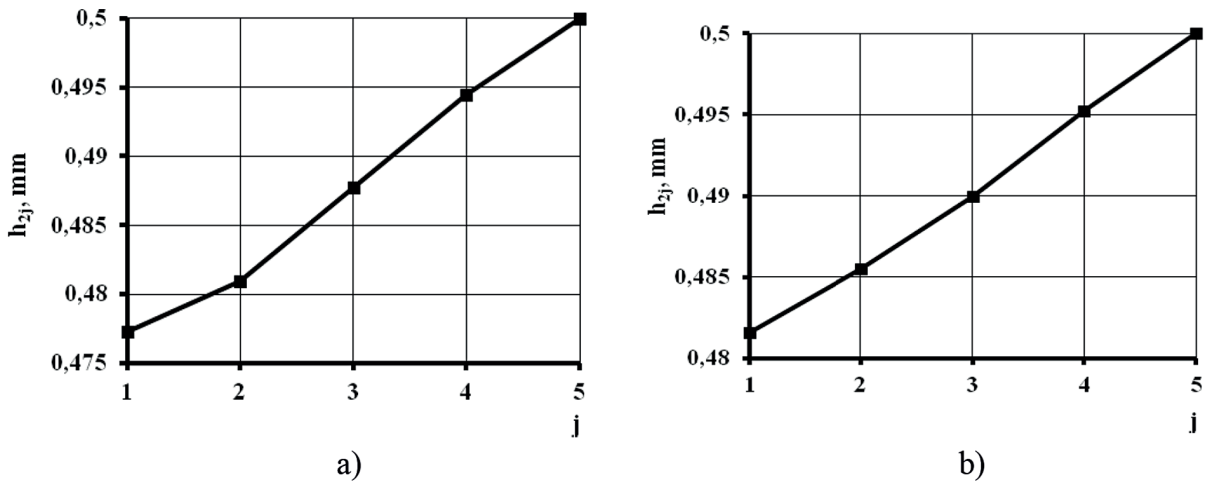**Fig. 10.** Minimum life of a PA6+30GF gear

Fig. 11. Linear wear of PA6 gear teeth along their profile
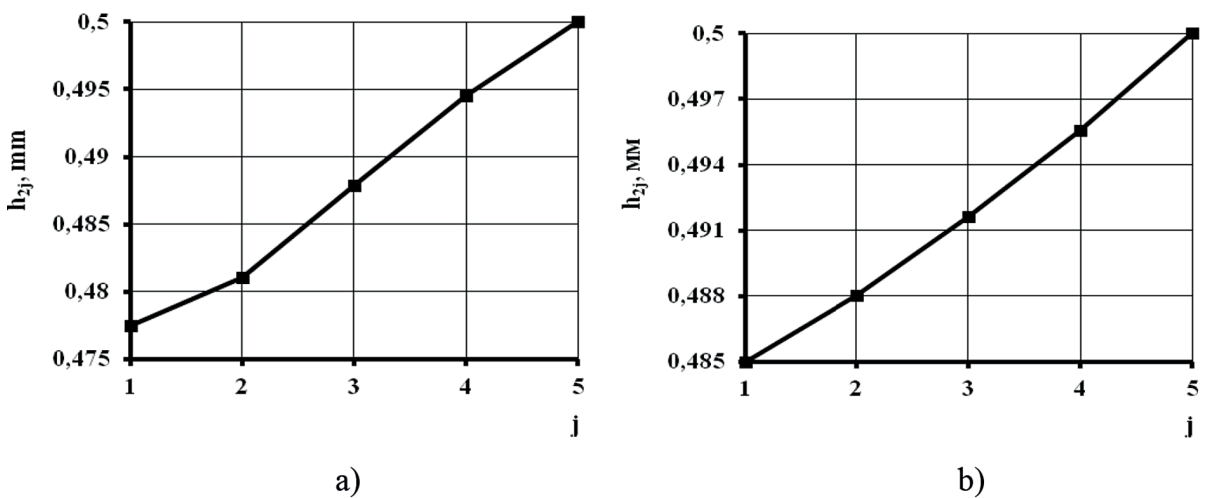

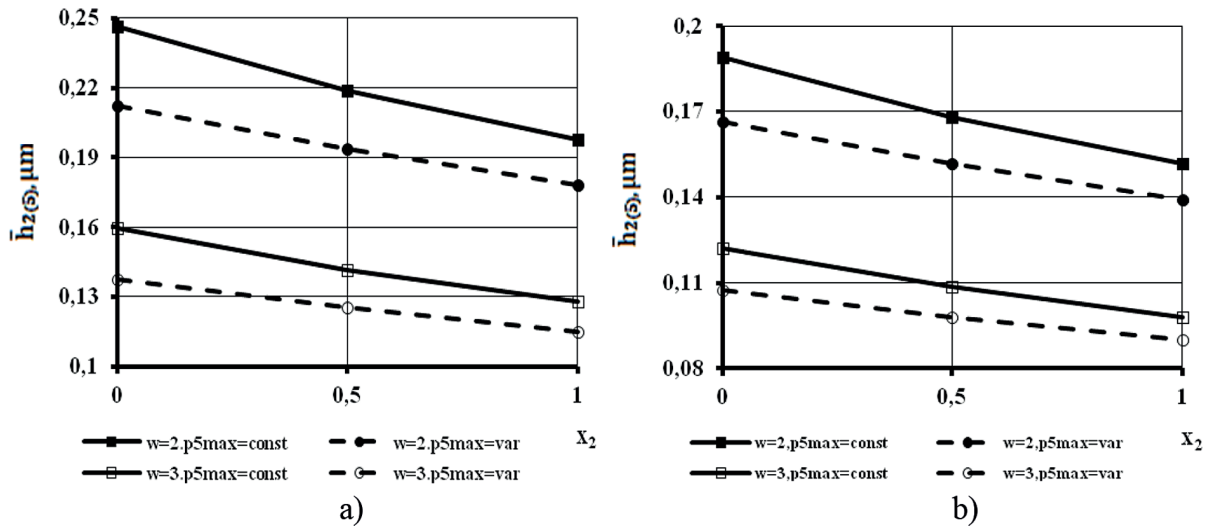**Fig. 12.** Linear wear of PA6+30GF gear teeth along their profile

Fig. 13. Linear wear of PA6 gear teeth after correction per one hour of operation
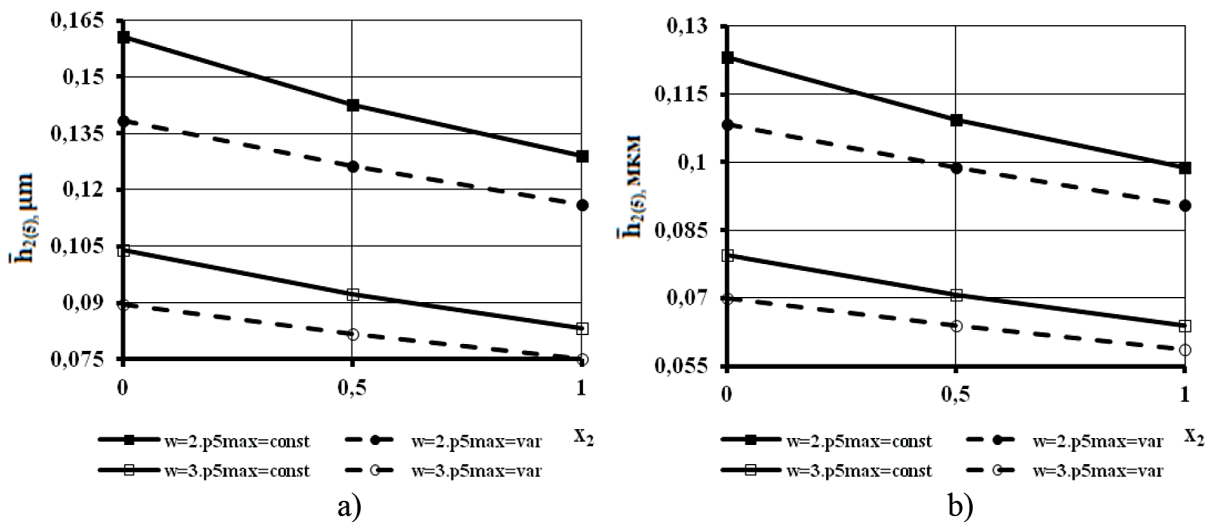

Fig. 14. Linear wear of PA6+30 GF gear teeth after correction per one hour of operation

CONCLUSIONS

According to the presented analytical method of testing metal-polymer involute and archimedes worm gears, quantitative and qualitative regularities of contact pressures in meshing, wear of non-metal worm gear teeth, gear service life were established.

It can be observed that the maximum contact pressure increases as the worm wheel teeth enter in mesh, which results from a decrease in equivalent curvature radius. The maximum contact pressure is located at the exit of engagement. The maximum contact pressure is significantly reduced due to the wear of worm wheel teeth. Worm wheel tooth correction leads to reduced contact pressures and increased gear life. The minimum gear life of the worm wheel teeth is observed at the exit of engagement, i.e. at tooth root. It is slightly higher at the addendum. An increase in tooth pairs in engagement from two to three leads to a considerable reduction in contact pressure and, at the same time, to a significant increase in gear life.

REFERENCES

1. Andreikiv A.Je. and Chernets M.V. Assessment of the Contact Interaction of Machine Parts in Friction [in Russian]. Kiev Naukova Dumka; 1991.

2. Chernets M. A method for predicting contact strength and life of Archimedes and involute worm gears, considering the effect of wear and teeth correction, Tribology in Industry. 2015; 1: 134–141.

3. Chernets M.V., Jarema R.J. Prediction of the life of

the worm gears in Archimedes and involute worm gears. Problems of Tribology. 2011; 2: 21–22.

4. Czerniec M., Kiełbiński J.: Prognozowanie trwałości tribologicznej kół zębatych walcowych ewolwentowych. Wyd. Politechniki Lubelskiej; 2003.

5. Chernets M.V. Prediction Method of Contact Pressures, Wear and Life of Worm Gears with Archimedean and Involute Worm, Taking Tooth Correction into Account, Journal of Friction and Wear. 2019; 4: 342–348.

6. Chernets M. Research of influence of engagement pairing of the corrected worm gear with involute worm on the life and contact pressure. Tribology in Industry. 2020; 42(3): 363–369.

7. Chernets M.V. Tribocontact tasks for cylindrical joints with technological non-circularity. Lublin Lublin University of Technology; 2013.

8. De Almeida Rosa A.G., Moreto J.A., Manfrinato M.D., Rossino L.S. Study on friction and wear behavior of SAE 1045 steel, reinforced nylon 6.6 and NBR rubber used in clutch disks. Mat. Res. 2014; 17(6): 1397–1403.

9. Gasparin A., L., Corso L. L., Tentardini E. K., Reis-Nunes R. C., de Camargo-Forte M., M., de Oliveira R., V.. Polyamide worm gear: manufacturing and performance. Mat. Res. 2012; 15(3): 483–489.

10. Gun-Hee K.1, Jeong-Won L. Tae-Il S. Durability Characteristics Analysis of Plastic Worm Wheel with Glass. Materials. 2013; 6: 1873–1890.

11. Hiltcher Y., GuingandM., de Vaujany J.P. Load Sharing of Worm Gear With a Plastic Wheel. J. Mech. Des. 2007; 129(1): 23–30.

12. Jbily D., Guingang M., de Vaujany J.P. Loaded behaviour of steel / bronze worm gear. International Gear Conference, Lyon Villenbanne, France 2014, 32–42.

13. Jbily D., Guingang M., de Vaujany J.P. A wear model for worm gear, J.MechEng. 2016; 230(7–8): 1290–1302.

14. Kalácska G. An engineering approach to dry friction behaviour of numerous engineering plastics with respect to the mechanical properties. eXPRESS Polymer Letters. 2013; 7(2): 199–210.

15. Kim S.H., Shin M. C., Won Byun J., Hwan K.O. Efficiency Prediction of Worm Gear with Plastic Worm Wheel. International Journal of Precision Engineering and Manufacturing. 2012; 13(2): 167–174.

16. Mithun V., Kulkarni K., Elagovan K., Hemachandra R., Basappa S. J. Tribological behaviours of ABS and PA6 polymer metal sliding combinations under dry friction, waterabsorbed and electroplated conditions. Journal of Engineering Science and Technology. 2016; 11(1): 12–18.

17. Palabiyik M., Bahadur S. Tribological studies of polyamide 6 and high-density polyethylene blends filled with PTFE and copper oxide and reinforced with short glass fibers. Wear. 2002; 253: 369–376.

18. Pogačnik A., Kupec A., Kalin M. Tribological properties of polyamide (PA6) in self-mated contacts and against steel as a stationary and moving body. Wear. 2017; 378–379: 17–26.

19. Sabiniak H.G. Wear and life of the worm gears. Publishing House of Lodz University of Technology: Lodz 2007.

20. Sharif K.J., Kong S., Evans H.P., Snidle R.W. Contact and elastohydrodynamic analysis of worm gears: Part 1 Theoretical formulation. Proc. Inst. Mech. Engrs, Part C: J. Mechanical Engineering Science. 2001; 215: 817–830.

21. Sharif K.J., Kong S., Evans H.P., Snidle R.W. Contact and elastohydrodynamic analysis of worm gears: Part 2 Rresults, Proc. Instn. Mech. Engrs, Part C: J. Mechanical Engineering Science. 2001; 215: 831–846.

22. Sharif K.J., Evans H.P., Snidle R.W., Barnett D., Egorov I.M., Effect of elasto-hydrodynamic film thickness on a wear model for worm gears, Proc Institutions Mechanical Enginers, Part J: Journal Engineering Tribology. 2006; 220: 295–306.

23. Sharif K.J., Evans H.P., Snidle R.W., Prediction of the wear pattern in worm gears, Wear. 2006: 261(5–6): 666–673.

24. Sharif K.J., Evans H.P., Snidle R.W. Wear modeling in worm gears. IUTAM Symposium on Elastohydrodynamic and Microelastohydro-dynamics. 2009; 134 (9): 371–383.

25. Snidle R.W., Evans H.P. Some aspects of gear, Mech. Eng. Science, 2009; 223(1): 103–114.

26. Yang F., Su D., Gentle C. R. Finite element modelling and load share analysis for involute worm gears with localized tooth contact. Proc. ImechE, Part C: Journal of Mechanical Engineering Science, 2001; 215: 805–816.

27. Zubrzycki J., Świć A., Taranenko W. Mathematical model of the hole drilling process and typical autom. ated process for designing hole drilling operations. Robotics in theory and practice. 2013: 221–229